2009

Triacylglyceride Metabolism by Fusarium graminearum During Colonization and Sexual Development on Wheat

John C. Guenther
Michigan State University

Heather E. Hallen-Adams
University of Nebraska at Lincoln, hhallen-adams2@unl.edu

Heike Bücking
South Dakota State University

Yair Shachar-Hill
Michigan State University

Frances Trail
Michigan State University, trail@msu.edu

MPMI Vol. 22, No. 12, 2009, pp. 1492–1503. doi:10.1094/MPMI-22-12-1492. *e*-Xtra*

Triacylglyceride Metabolism by *Fusarium graminearum* During Colonization and Sexual Development on Wheat

John C. Guenther,[1] Heather E. Hallen-Adams,[1] Heike Bücking,[2] Yair Shachar-Hill,[1] and Frances Trail[1,3]

[1]Department of Plant Biology, Michigan State University, East Lansing, MI 48824, U.S.A.; [2]Biology and Microbiology Department, South Dakota State University, Northern Plains Biostress, Brookings, SD 57007, U.S.A.; [3]Department of Plant Biology and Department of Plant Pathology, Michigan State University, East Lansing, MI 48824, U.S.A.

Submitted 21 May 2009. Accepted 7 August 2009.

***Fusarium graminearum*, a devastating pathogen of small grains, overwinters on crop residues and produces ephemeral perithecia. Accumulation of lipids in overwintering hyphae would provide reserves for overwinter survival and perithecium development. Fatty acid composition of cultures during perithecium development indicated a drop in neutral lipid levels during development but little change in fatty acid composition across stages. Microscopic examination of cultures early in sexual development revealed hyphal cells engorged with lipid bodies. In comparison, vegetative hyphae contained few lipid bodies. Microarray analysis was performed on wheat stems at stages of colonization through perithecium development. Gene expression analysis during stages of perithecium development both in planta and in vitro (previously published) supports the view that lipid biosynthesis occurs during early stages of wheat colonization leading to sexual development and that lipid oxidation occurs as perithecia are developing. Analysis of gene expression during the stages of wheat stem colonization also revealed sets of genes unique to these stages. These results support the view that lipids accumulate in hyphae colonizing wheat stalks and are subsequently used in perithecium formation on stalk tissue. These results indicate that extensive colonization of plant tissue prior to harvest is essential for subsequent sporulation on crop residues and, thus, has important implications for inoculum reduction.**

Fusarium graminearum Schwabe (teleomorph *Gibberella zeae* (Schwein.) Petch) causes head blight of wheat, barley, and oat and foot rot of corn. The grain from infected plants is frequently contaminated by mycotoxins, including deoxynivalenol, fusarin C, and zearalenone (Trail 2009), resulting in reduced grain quality in addition to yield losses. Both sexual (ascospores) and asexual (macroconidia) propagules are produced by *F. graminearum* but ascospores are generally believed to be the primary inoculum of the disease (Shaner 2003). Ascospores are produced in flask-shaped fruiting bodies called perithecia and are forcibly discharged into the air to facilitate dispersal. The period of flowering is the most susceptible stage of wheat for head blight, and dispersal of ascospores during this period provides a major target for designing new control methods. Disease was significantly reduced following the seeding of wheat field plots with a genetically engineered strain that fails to produce ascospores (Desjardins et al. 2006). Recent studies demonstrated that sexual development in *F. graminearum* is initiated during plant colonization (Guenther and Trail 2005). In infected wheat, small hyphal coils, termed perithecium initials, are formed in association with stomates and silica cells as the plant tissue senesces. The initials and associated hyphae, which subtend the epidermis and link the initials, are the overwintering structures which generate perithecia (Guenther and Trail 2005) during periods of moderate temperatures and moisture (Chen and Yuan 1984; Reis 1990; Trail et al. 2002; Inch et al. 2005).

In fungi, lipids are known to be involved in cold tolerance and survival (Istokovics et al. 1998); cell wall dynamics (Bagnat et al. 2000); carbon translocation (Bao et al. 2002); plant–pathogen interactions (Cheng et al. 2004), including appressorium function in *Magnaporthe grisea* (Ramos-Pampiona and Naqvl 2006; Wang et al. 2007); cell signaling (Carpenter and Ji 1999); and regulation of cellular growth and development (Calvo et al. 1999, 2001 Dyer et al. 1993). Fungi secrete lipases that break down lipids into fatty acid components. These are then taken up and used directly or broken down further for energy or to generate acetyl CoA, which is a precursor for the synthesis of some secondary metabolites and for other cellular pathways. Lipids destined for storage are packaged into lipid bodies (Pfeffer et al. 1999; Bago et al. 2002), dynamic structures in close association with cell membranes (Murphy and Vance 1999; Tsitsigiannis et al. 2004), where they function in maintaining membranes and membrane composition changes, and as a source of stored energy. Lipid stores are predominantly composed of triacylglycerides, which are characterized by a glycerol backbone and three fatty acyl side chains. The fatty acyl side-chains vary (Murphy 2001) and their composition tends to be species specific (Weete 1974).

The demonstration that perithecium initials arise during colonization of infected plants (Guenther and Trail 2005) suggests that the production of ascospores may be influenced by preharvest colonization. Because ascospores are considered important to the epidemiology of the disease, consideration of the development of the sexual stage is critical. Colonization of infected stems leading to perithecium development was previously characterized (Guenther and Trail 2005). Three discrete infection stages were identified. i) The infection front (IF) was characterized by narrow, uninucleate vegetative hyphae which move through the pith and vascular elements asymptomatically. ii) Behind the front, hyphae in the xylem and pith are

J. C. Guenther and H. E. Hallen-Adams contributed equally.

Corresponding author: F. Trail; E-mail: trail@msu.edu

Current address of J. C. Guenther: Neogen Corporation, Lansing, MI 48912, U.S.A.

*The *e*-Xtra logo stands for "electronic extra" and indicates that a supplementary table is published online.

wide and binucleate, sending out radial hyphae (RW), morphologically similar to those at the front, which colonize the chlorenchyma tissue, causing visible necrosis. iii) Behind the RW region, the wheat takes on the bleached appearance characteristic of the disease. This senesced wheat (SW) harbors perithecium initials beneath the stomates. These three stages are found simultaneously on infected plants as the infection front progresses down the stem.

Previously, lipids were observed in culture in association with perithecium initials (Trail and Common 2000). We hypothesize that the accumulation of lipids precedes the energy-intensive process of fruiting body development and sporulation, is essential for overwinter survival and perithecium production on crop residues, and therefore, is an important part of the disease cycle of this pathogen. Thus, procuring host carbon resources prior to host senescence would allow the fungus to sequester the maximum resources for overwinter survival and subsequent sporulation. We investigated fatty acid composition of cultures during sexual development and gene expression during perithecium development in infected wheat stalks and in vitro. In addition, we investigated sugar utilization of growing vegetative hyphae to determine the preferred sugar sources for fungal growth and, thus, those sources that are most likely converted into lipids in planta. Our results reveal that sexual development is initiated in association with colonization of the wheat plant prior to harvest, and that this initial colonization will largely determine the inoculum produced in the subsequent disease cycle.

RESULTS

Triacylglyceride profiles in the life cycle of *F. graminearum*.

To characterize the lipid content and composition of life cycle stages, ^{1}H-nuclear magnetic resonance (NMR) analysis was performed on neutral lipids extracted from aerial vegetative hyphae (0 h) and surface mycelia in cultures at 24 h (binucleate stage and perithecium initials), 48 h (very young perithecia), and 96 h (immature asci within the perithecia). (For a description of all stages, discussed below). The ratio of the area of methyl peaks to the sum of glycerol peak areas was 9.27:5.03 for all samples, affirming that the majority of the fatty acids in the neutral lipid extract were associated with glycerol, and mainly as triacylglycerides (TAG) (data not shown) (a ratio of 9:5 methyl/glycerol would indicate that all fatty acids are associated with TAG.)

To determine the fatty acid composition of TAGs accumulating during these developmental stages, derivatized fatty acid methyl esters were analyzed by gas chromatography (GC)-flame ionization detection spectra (FID) (Table 1). The largest proportion of the lipid present in vitro was composed of C18:1 fatty acids, followed by C18:2 and C16:0. Vegetative aerial hyphae and 48-h cultures contained a higher percentage of extractable nonpolar lipids, in the form of TAG, than did the 24- or 96-h stages. The 96-h sample showed a higher relative proportion of C18:2 to C18:1 compared with other time points. Wheat stem samples, whether infected or not, contained very low quantities of TAG, less than 1% oil by weight (results not shown). The component contributed by fungi would be a fraction of this; therefore, these data were not analyzed further.

Visualizing lipid storage in hyphae.

Hyphae were examined for the presence of lipid bodies in culture. Synthetic crossing (SC) medium is transparent and allowed the ready identification of developmental stages for dissection. Lipid bodies are diffuse in vegetative hyphae but fill cells in the wider hyphae that are characteristic of mature cultures leading to sexual reproduction (Fig. 1). Lipid bodies were consistently observed to be associated with wider hyphae

Table 1. Fatty acid composition of neutral lipids in culture determined by gas chromatography flame ionization detection[a]

Treatment	C16:0	C16:1	C18:0	C18:1	C18:2	C18:3	Oil by weight (%)
Carrot agar (control)	18.9	ND	9.0	4.2	63.7	4.2	0.2
Aerial vegetative hyphae	20.1	0.63	9.2	46.5	20.7	2.9	7.5
24 h	17.9	ND	10.8	43.1	25.0	3.2	3.3
48 h	19.0	0.84	8.0	46.2	23.1	3.0	7.3
96 h	17.2	ND	8.3	41.2	30.6	2.8	2.9

[a] ND = not detected.

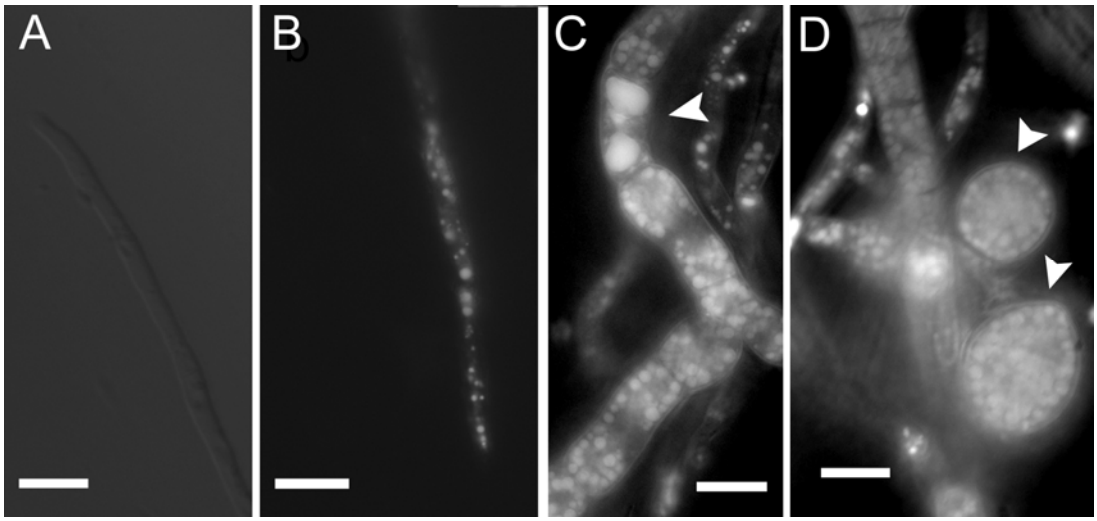

Fig. 1. Lipid accumulation in hyphae. **A,** Aerial vegetative hypha; unstained overexposure. **B,** Aerial vegetative hyphae, 0 h. **C,** Hypha embedded in synthetic crossing medium. Damaged cell results in lipid coalescence (arrowhead). **D,** Perithecium initials (arrowheads) erupting from lipid dense mycelia. Samples stained with Nile Red unless otherwise indicated. Fluorescence observed as described in text. Size bars = 10 μm.

in mature cultures on carrot agar over several years, with >100 independent observations. We recently determined that the background fluorescence common in carrot agar, due to the presence of plant material, could be eliminated by growing these stages on SC medium. In addition, SC medium does not require induction for formation of the sexual stage, nor does it have an endogenous source of lipids. Therefore, we can conclude that the source of the lipids in hyphae on SC medium were synthesized de novo.

Gene expression analysis in wheat stalks.

Previously, transcript accumulation was analyzed during perithecium development in culture (Hallen et al. 2007). To compare gene expression of the development of these stages in

Table 2. Genes analyzed for expression throughout triglyceride biosynthesis and degradation

No.[a]	FGSG number[b]	EC	Annotation
Fatty acid biosynthesis			
1	FGSG_02502	1.14.19.1	Probable sterol delta 5,6-desaturase
2	FGSG_04994	1.14.19.1	Probable sterol delta 5,6-desaturase
3	FGSG_05321– – –	2.3.1.85	Probable fatty acid synthase, α subunit
4	FGSG_05322– – –	…	Probable fatty-acyl-CoA synthase, β subunit
5	FGSG_06039–	2.3.3.8	Probable ATP citrate lyase subunit 2
6	FGSG_06184– – –	1.14.19.1	Probable stearoyl-CoA desaturase
7	FGSG_06580– –	6.4.1.2	Probable acetyl-CoA carboxylase
8	FGSG_07890– –	1.14.19.1	Probable bifunctional D12/D15 fatty acid desaturase
9	FGSG_08329–	6.3.4.15	Related to BPL1–biotin holocarboxylase synthetase
10	FGSG_12857–	2.3.3.8	Probable ATP citrate lyase subunit 1
Triglyceride biosynthesis			
11	FGSG_05023– –	1.1.1.8	Probable glycerol-3-phosphate dehydrogenase (NAD)
12	FGSG_06642	2.3.1.51	Related to sn2-acylglyceride fatty acyltransferase
13	FGSG_06688– –	2.3.1.20	Related to diacylglycerol acyltransferase
14	FGSG_13398– –	2.3.1.16	Probable acetyl-CoA C-acyltransferase precursor
Fatty acid β-oxidation			
15	FGSG_00407	1.3.1.34	Probable 2,4-dienoyl-CoA reductase SPS19
16	FGSG_00704+	4.2.1.17	Related to probable enoyl-CoA hydratase
17	FGSG_01419+	6.2.1.3	Related to long-chain-fatty-acid CoA ligase FAA2
18,	FGSG_02287	…	Related to POX1–acyl-CoA oxidase
19	FGSG_05140	1.3.99.3	Related to acyl-CoA dehydrogenase, medium-chain specific, mitochondrial precursor
20	FGSG_05872	4.2.1.17	Related to enoyl-CoA hydratase
21	FGSG_09424	6.2.1.3	Related to long-chain fatty-acid-CoA ligase
22	FGSG_09643+	…	Probable multifunctional β-oxidation protein
23	FGSG_09661++	1.3.99.3	Probable acyl-CoA dehydrogenase short-branched chain precursor
24	FGSG_10285+	1.3.99.10	Related to acyl-coa dehydrogenase, long-chain specific precursor
25	FGSG_10790	1.3.99.3	Probable acyl-CoA dehydrogenase
26	FGSG_12049	1.1.1.157	Related to 3-hydroxyacyl-CoA dehydrogenase
27	FGSG_13860+	6.2.1.3	Related to phenylacetyl-CoA ligase
Triglyceride degradation			
28	FGSG_01571+	3.1.1.79	Related to hormone-sensitive lipase
29	FGSG_01603+++	3.1.1.3	Probable triacylglycerol lipase V precursor
30	FGSG_01975	3.1.1.3	Related to triacylglycerol lipase
31	FGSG_03247	2.7.1.30	Probable GUT1–glycerol kinase
32	FGSG_05906++	3.1.1.3	Probable triacylglycerol lipase precursor
33	FGSG_07468	1.1.1.95	Probable SER33–3-phosphoglycerate dehydrogenase
34	FGSG_10713+	3.1.1.3	Related to triacylglycerol lipase V precursor
35[c]	FGSG_13343++	2.7.1.30	Probable GUT1–glycerol kinase
36	FGSG_13655+	3.1.1.3	Related to triacylglycerol lipase V precursor
Glycolysis			
37	FGSG_00500	2.7.1.1	Probable hexokinase
38	FGSG_08399	2.7.1.1	Related to hexokinase
39	FGSG_09456	2.7.1.11	Probable 6-phosphofructokinase
Associated reductants			
40	FGSG_00805	1.1.1.38	Probable malate dehydrogenase (oxaloacetate decarboxylating) (NADP+)
41	FGSG_02461	1.1.1.37	Probable MDH1–malate dehydrogenase precursor, mitochondrial
42	FGSG_03174– –	1.1.1.93	Related to LYS12–homo-isocitrate dehydrogenase
43	FGSG_07191++	1.1.1.40	Related to malate dehydrogenase (oxaloacetate-decarboxylating) (NADP+)
44	FGSG_10347–	1.1.1.42	Probable IDP1–isocitrate dehydrogenase (NADP+), mitochondrial
Other sugars			
45	FGSG_02339	…	Related to SUC2–invertase (sucrose hydrolyzing enzyme)
46	FGSG_04826	1.1.1.184	MTDH1 mannitol dehydrogenase
47	FGSG_05697–	2.4.1.15	Related to α,α-trehalose-phosphate synthase (UDP-forming)
48	FGSG_06051	2.4.1.15	Probable TPS1–α,α-trehalose-phosphate synthase, 56 KD subunit
49	FGSG_07926	3.1.3.12	TPS2 probable trehalose-6-phosphate phosphatase
50	FGSG_12827	1.1.1.17	M1PD probable mannitol-1-phosphate dehydrogenase
Glyoxylate cycle			
51	FGSG_08700–	…	Probable DAL7–malate synthase 2
52	FGSG_09896	…	Probable isocitrate lyase (acu-3)

[a] Numbers corresponding to Figure 2.

[b] + and – = 2- to 4-fold up- or downregulation, respectively, at 48 h compared with 24 h; ++ and – – = 4-fold to 20-fold up- or downregulation, respectively, at 48 h compared with 24 h; and +++ and – – – = 20-fold or greater up- or downregulation, respectively, at 48 h compared with 24 h.

[c] Appears twice in Figure 2, due to the existence of two probesets for this gene.

the host, we performed transcriptome analysis during stem colonization in wheat using the Fusarium GeneChip. Here, we have focused on a set of genes representing enzymes involved in fatty acid biosynthesis, triacylglyceride biosynthesis, and fatty acid and triacylglyceride oxidation (Table 2). The expression of these genes was monitored across a sexual developmental series. The normalized transcript data were used to establish apparent patterns of expression for TAG biosynthesis and oxidation through developmental time courses in planta and in vitro (Figs. 2 and 3). In general, accumulation of transcripts for genes associated with TAG generation was counter to the accumulation for genes associated with TAG breakdown.

To better understand transcript accumulation throughout the perithecium development process in culture and in wheat stems, we conducted a cluster analysis for 52 genes significant to lipid accumulation (Fig. 2). This analysis generated a false-color plot that reordered rows according to row means, giving a dendrogram for rows (genes tested) only. Columns represent treatments with repetitions and were not reordered. Rows were scaled to have a mean of 0 and standard deviation of 1. This statistical treatment better illustrates the pattern of expression but not the intensity or real value of expression of individual genes. Several interesting patterns can be observed in the resultant heat map (Fig. 2). Lipid biosynthesis genes and lipid oxidation genes clustered generally into separate branches. The majority of lipid biosynthesis genes clustered into a major group (Fig. 2, group 1), revealing increased messenger (m)RNA accumulation at the early stages of culture and during stem colonization. Four smaller groups were formed, with groups 2 and 4 composed primarily of oxidation genes and group 3 primarily of biosynthetic genes. Group 5 is composed of genes from both sets. A distinct similarity can be determined between false-color assignments for 0 and 24 h and IF, RW, and SW phases of wheat stem treatments for each row. The greatest change in expression for all gene sets occurred between 24 to 48 h in culture treatments and, for the analogous stages in planta, between SW and "young perithecia" (YP).

Transcript abundance for genes related to lipid biosynthesis in culture was characterized by a significant increase in transcripts at 24 h and a significant decrease in transcripts begin-

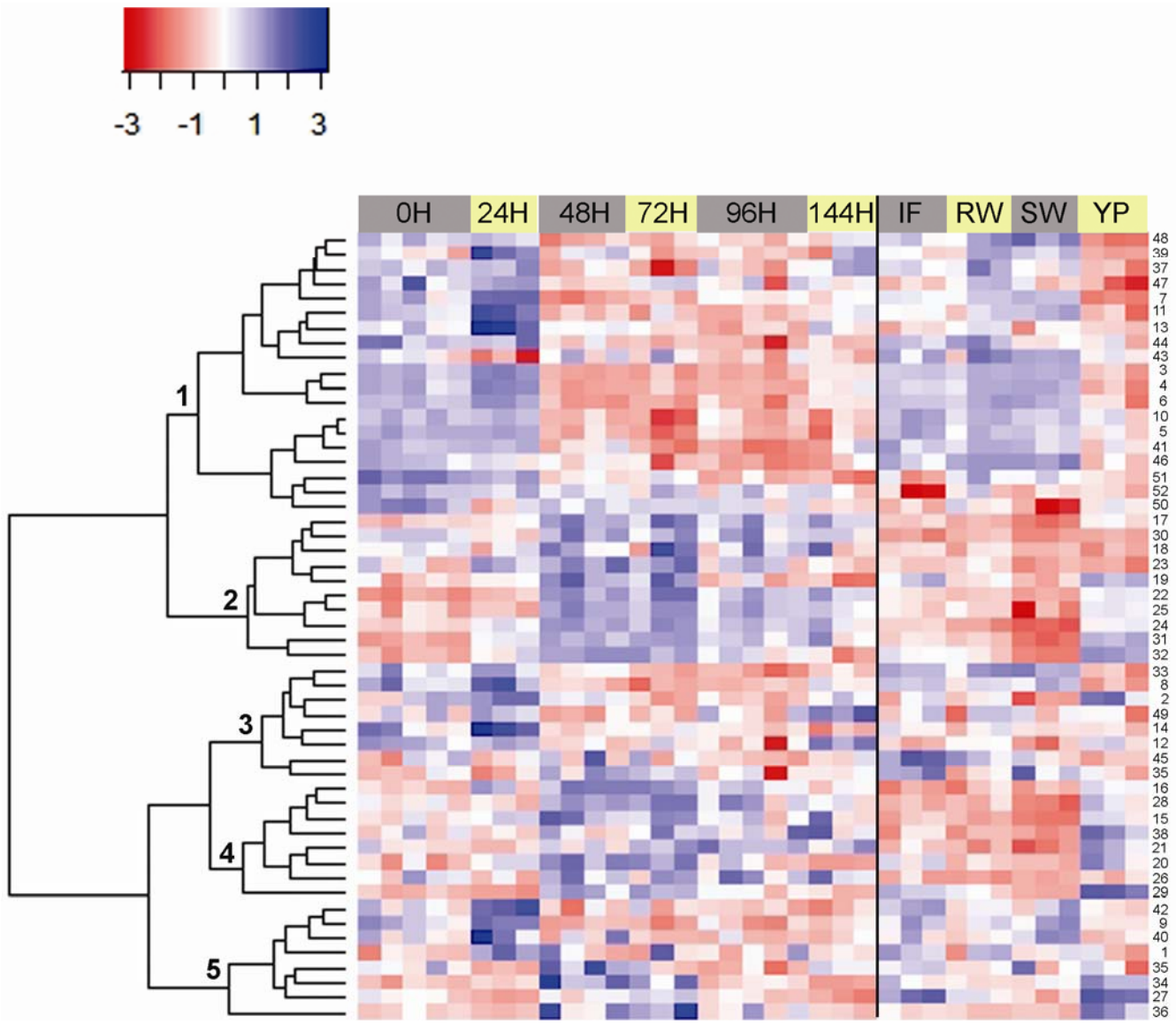

Fig. 2. Expression profiles throughout perithecium development of metabolic genes selected for their role in lipid biosynthesis and lipid oxidation. Expression data both in vitro (left of black bar) and in vivo (right of black bar) are presented. IF (infection front); RW (water-soaked wheat); SW (senesced wheat); YP (after harvest, stem in moisture to induce perithecium development). Perithecium developmental stages (0 to 144 h) in vitro are described in the text. Groups are indicated at left; numbers at right correspond to genes in Table 2.

ning at 48 h compared with 0 h. Of the 16 genes analyzed for lipid biosynthesis, 10 showed twofold or greater increase in transcript levels at 24 h compared with 0 h (Fig. 2). Of the 16 genes, 14 showed a statistically-significant decrease of 2-fold or greater at 48 h compared with 24 h (Table 2), at P values < 0.004; the greatest changes were observed in the probable fatty acid synthase, α-subunit gene FGSG_05321 and the probable stearoyl-CoA desaturase gene FGSG_06184, both of which showed a 38-fold decrease at 48 versus 24 h. These results are representative of an observed pattern of transcript accumulation that was consistent for genes throughout the lipid biosynthesis pathway and throughout perithecium development. Of the 22 genes involved in lipid oxidation, only 4 decreased by greater than twofold after 24 h and only one of these decreases was statistically significant.

For genes involved with lipid oxidation, transcript accumulation in culture at 48 h increased significantly compared with 0 h. Of the 22 genes involved in the oxidation of lipids, 13 showed an increase in transcript levels greater than twofold at 48 h compared with 0 h (Table 1). Of these 22 genes, 14 showed a statistically significant increase of 2-fold or greater at 48 h compared with 24 h (P values < 0.004); the greatest change was a 20-fold increase in transcript abundance of probable triacylglycerol lipase V precursor gene FGSG_01603. Triglyceride lipases disassemble TAG, releasing fatty acids and glycerol. Acyl-CoA dehydrogenase and enoyl-CoA dehydratase are enzymes within the β-oxidation pathway. The pattern of transcript flux for these genes was characteristic of those observed for lipid oxidation (Fig. 3).

Additionally, we used quantitative reverse-transcript polymerase chain reaction (qRT-PCR) to evaluate expression of four genes from across the in vitro time course: two representative biosynthesis genes (FGSG_05321, fatty acid synthase and FGSG_05609, triacylglycerol lipase) and two representative β-oxidation genes (FGSG_06039, ATP citrate lyase, and FGSG_10790, acyl-CoA dehydrogenase). Gene expression (as cycle threshold [Ct] values) was normalized to that of glyceraldehyde phosphate dehydrogenase (GAPDH, a housekeeping gene; FGSG_6257). The expression profiles mirrored those observed on the Affymetrix gene chips, with the β-oxidation genes exhibiting moderate expression at 0 h, higher expression at 24 h, and highest expression at 48 and 72 h, followed by a decline in expression levels. Likewise, the biosynthesis gene expression patterns reflected those observed on the GeneChip.

We examined the FunCat categories of genes expressed uniquely in each of the in planta stages and compared them with the in vitro sexual development series, and to previously published in vitro and barley infection studies (Gueldener et al. 2006). Strikingly, the FunCat categories that were expressed at significantly higher representation across IF, RW, and SW re-

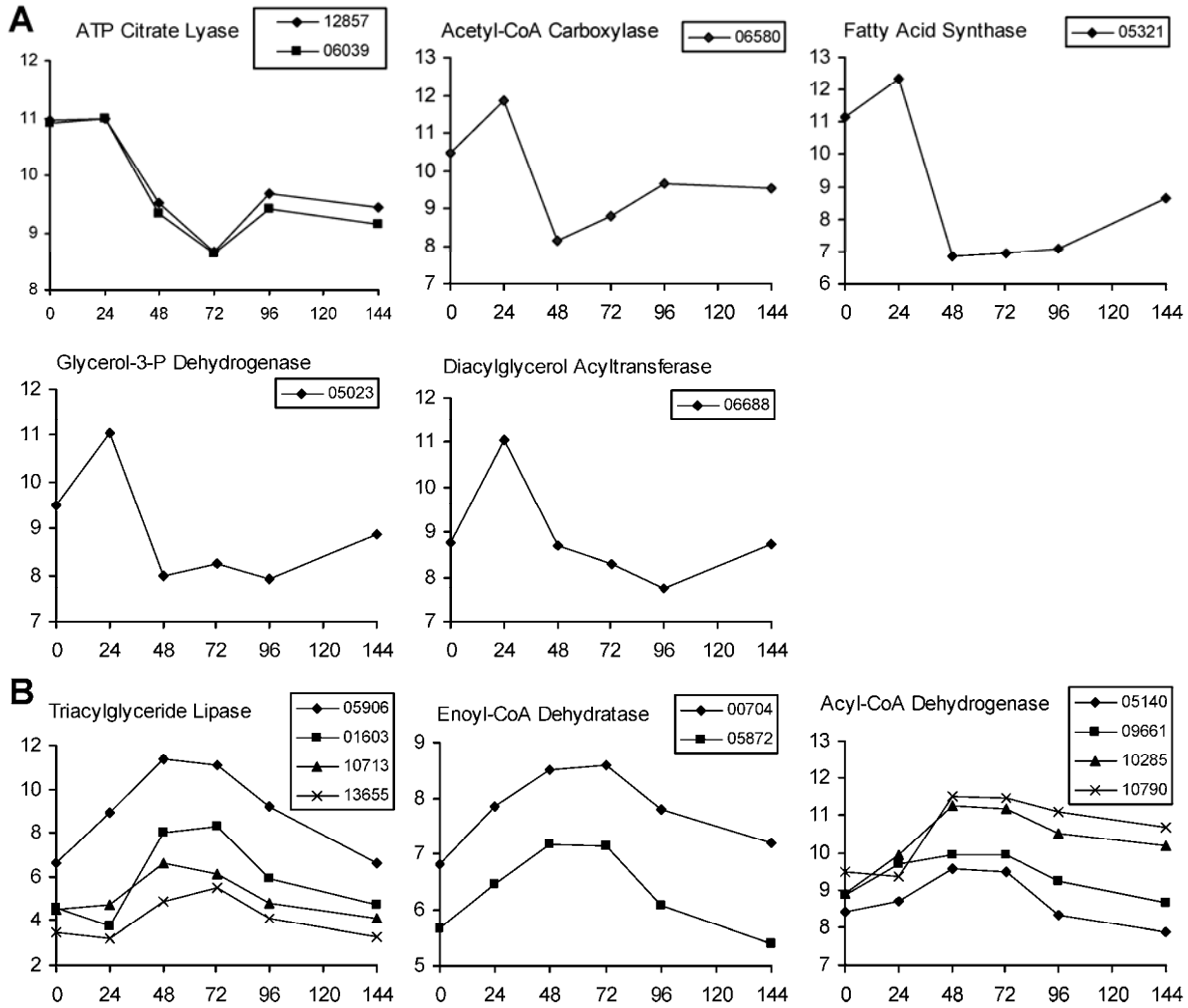

Fig. 3. Transcript accumulation of lipid biosynthesis and lipid oxidation genes in culture. **A,** Characteristic transcript level of genes involved in fatty acid and triacylglyceride biosynthesis. **B,** Transcript accumulation pattern of genes involved with triacylglyceride oxidation. Plots represent $\log_2$ normalized transcript accumulation verses hours post induction. Numbers correspond to the FGSG gene numbers in MIPS annotation build FG3.

lated to sugar metabolism, fatty acid metabolism, secondary metabolism, and genes related to disease, virulence, and defense (Supplementary Table S1). In brief, 416 probesets were uniquely detected only in planta (regardless of stage or host) and not in any in vitro stage and 234 probesets were detected in wheat but not barley. However, because the barley data were collected at early head infection, this does not necessarily indicate that these genes are host specific. Categories significantly overrepresented in wheat included extracellular metabolism (FunCat 01.25); secondary metabolism (FunCat 01.20); disease, virulence, and defense (FunCat 32.05); detoxification by degradation (FunCat 32.07.09); and C-compound and carbohydrate metabolism (FunCat 01.05).

Sugar uptake and utilization in *F. graminearum*.

To begin to understand how carbon nutrition leads to lipid accumulation, we examined the uptake of simple sugars that are available to the fungus during host colonization. Sucrose, glucose, and fructose are the sugars commonly available in crop tissue (Acevedo et al. 1979; Jones et al. 1980) and have been shown to accumulate to higher levels in wheat, particularly during drought stress (Kameli and Losel 1996), a condition which may be imposed on wheat by *F. graminearum* infection due to the plugging of xylem vessels (Guenther and Trail 2005). Therefore, these sugars were used in a study to determine which were most readily absorbed by the fungus. When sucrose was supplied, the carbon uptake was two to three times higher when compared with glucose or fructose (Fig. 4). After 144 h of mycelial growth, 27.3 ± 0.5 or 24.3 ± 0.5% of the supplied sucrose (high or low concentrations, respectively) was taken up by the fungus, but only 10.5 ± 0.2% of fructose and 7.4 ± 0.6% of glucose was taken up. A significant uptake from the medium after sucrose addition was detected 8 to 24 h after the addition, whereas a significant uptake of fructose or glucose was first visible after 72 and 96 h, respectively.

A GC-mass spectrometry (MS) profile of the simple sugars present during early development of perithecia was performed on cultures grown on carrot agar (Table 3). Samples were collected from uninoculated carrot agar (control), vegetative mycelia, and induced cultures. The predominant sugars in carrot agar were fructose, glucose, and sucrose. Predominant sugars extracted from fungal tissue were galactose, mannitol, and trehalose. At 96 h, trehalose, a major fungal storage disaccharide, had the highest relative level of the three predominant sugars. Wheat stems colonized by the fungus showed shifts in sugar content compared with uninoculated stems. The relative amount of sucrose declined in the senesced tissue samples whereas the fructose and mannitol content in senesced samples was almost twofold higher than in the controls. Mannitol and trehalose were minor sugars in the infected stems, in contrast

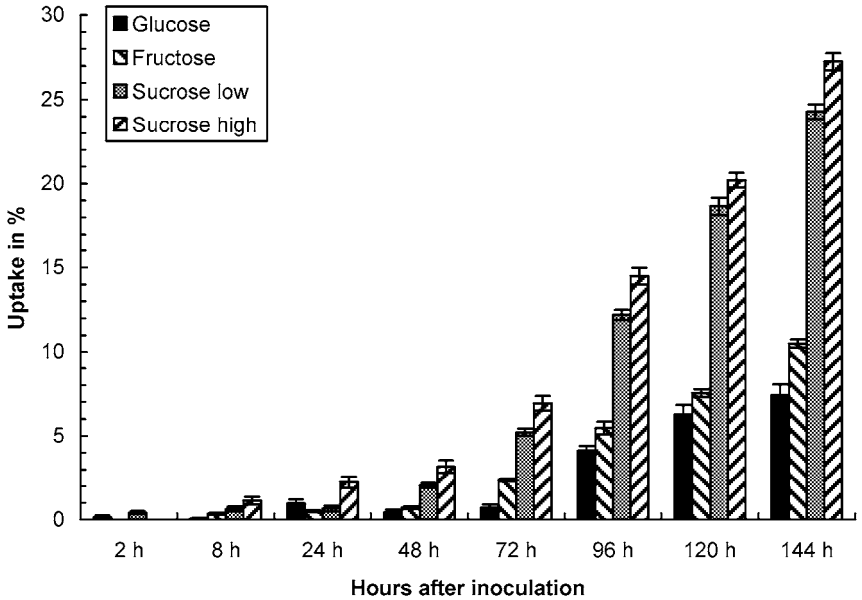

Fig. 4. Uptake of ^{14}C-glucose, ^{14}C-sucrose, and ^{14}C-fructose by *Fusarium graminearum* in liquid culture. The initial concentration of each sugar was 55.49 mM glucose, 55.49 mM fructose, and 29.21 mM (low) or 55.49 mM (high) sucrose.

Table 3. Sugar composition (%) of water soluble extracts in culture as determined by gas chromatography–mass spectrometry[a]

Treatment	Fruc	Gluc	Suc	Gal	Inos	Man	Tre	Glyc	Mal
In culture									
Carrot agar	24.9	38.5	25.7	5.3	1.1	0.4	ND	0.4	3.6
Vegetative aerial hyphae	0.7	3.7	ND	18.6	3.1	47.2	24.7	1.6	0.5
24 h	7.8	1.2	ND	15.7	2.3	55.1	15.2	2.1	0.5
48 h	0.3	0.7	ND	20.8	4.2	52.1	19.5	0.5	1.9
96 h	0.4	1.3	ND	18.3	2.4	34.2	41.2	1.8	0.4
In planta									
Control	18.8	23.3	47.3	ND	ND	2.8	ND	7.9	ND
Infection front[b]	23.3	16.1	41.1	ND	ND	3.0	1.9	8.0	6.6
Senesced	32.8	16.5	28.0	ND	ND	7.9	3.0	7.8	4.0

[a] Values are expressed as a percentage of sugar in the water-soluble extract for each treatment. Fruc = fructose, Gluc = glucose, Suc = sucrose, Gal = galactose, Inos = inositol, Man = mannitol, Tre = trehalose, Glyc = glycerol, Mal = maltose, and ND = not detected.

[b] For this study, infection front included the radial region because the radial region alone provided insufficient material for analysis.

to the culture samples, as would be expected due to the relatively low proportion of fungal biomass in the infected stems. NMR spectra of culture samples confirmed the findings from GC-MS (not shown).

DISCUSSION

The results presented here suggest that lipid accumulation precedes sexual reproduction and that oxidation of lipids accompanies fruiting body development. In addition, in vitro observation of hyphae suggests that lipid bodies accumulate preferentially in the specialized hyphae that support perithecium development. Expression of genes involved in lipid biosynthesis and lipid oxidation, both in vitro and in planta, supports this view. The results suggest that the extensive colonization of plant tissue prior to harvest is important to subsequent sporulation on crop residues and indicate that secondary saprotrophic invasion of crop residues may not be important to development of ascospore inoculum.

Genes involved in lipid biosynthesis are highly expressed during vegetative growth and early sexual development in culture, and during colonization in wheat stalks. Conversely, genes involved in β-oxidation showed higher transcript levels during sexual development in both culture and wheat stalks, when lipids would be used for energetics and building cellular structures. Gene expression analysis suggests two phases of cellular growth with respect to lipid metabolism: a biosynthetic phase, where lipids are synthesized and accumulate, and a phase during which stored lipids are utilized to produce fruiting bodies. Microscopic observations of growth in vitro confirmed a phenotypic change in hyphal development that was accompanied by formation of numerous lipid bodies as the cultures developed (Fig. 1). Estimates of fatty acid content by dry weight of the developmental stages do not follow this distinctive pattern but show a lower relative amount of fatty acids in the 24- and 96-h samples and a relatively higher content in the vegetative aerial and 48-h samples (Table 1). Because hyphae are removed at induction (0 h), the lower relative fatty acid content of the 24-h samples may reflect the removal of hyphae (and lipid stores contained therein) during the period of accumulation, resulting in a loss of accumulated lipid that would not occur in nature. Accumulation of lipid reserves during early stages of development (through 48 h) would fuel the energy-intensive sexual development state, reflected in the drop in lipid content at 96 h.

In planta, sucrose is present in the uninfected plants in the highest quantities, with glucose and fructose at approximately half the concentration (Table 3). Sucrose is the main transport sugar in plants and, therefore, the major carbon source for plant pathogens and, in the feeding studies (Fig. 4), the utilization of sucrose was much faster than glucose or fructose. Sucrose may be preferentially transported into the fungal cells, possibly due to early expression of sucrose transporters, or it may be rapidly hydrolyzed by extracellular invertases, and the resulting monosaccharides would then be taken up by the cell. We found that, in infected stem tissue, the sucrose contents decreased whereas the fructose contents steadily increased over time (Table 3). Ikeda and associates (1955) also showed that infected florets of wheat and barley had increased concentrations of glucose and fructose. This suggests that sucrose is first hydrolyzed by an apoplastic invertase and glucose is preferentially taken up. However, our sugar uptake studies (Fig. 4) indicated that glucose and fructose are taken up similarly with a slight preference for fructose. Glucose and fructose are taken up by a common hexose transporter in *Pyrenopeziza brassicae* (Walters et al. 1996), and a fungal hexose transporter has been identified that is specifically localized in the haustorial plasma membrane of *Uromyces fabae* (Voegele et al. 2001). The fructose uptake by this transporter is strongly reduced when glucose is present, and this might explain why glucose is preferentially taken up in infected plant tissue but not in our uptake studies, in which the different carbon sources were supplied separately. *F. graminearum* has 22 predicted hexose transporters (Munich Information Center for Protein Sequences [MIPS] database) whose various roles and specificities have yet to be determined.

It has long been known that the invertase activity increases in response to biotic stress (Wright et al. 1995) but it has been difficult to distinguish whether the observed increase is of plant or of fungal origin. Recently, Voegele and associates (2006) characterized a novel invertase from the obligate biotroph *U. fabae* that is transcribed during leaf penetration and that is highly expressed in fungal haustoria. *F. graminearum* has three putative invertases: an extracellular invertase (FGSG_08415), an intracellular invertase (FGSG_03288), and a gene related to the *Saccharomyces cerevisiae* invertase gene, *Suc2* (FGSG_02339) (Carlson and Bodstein 1982). *Suc2* in yeast encodes an intracellular invertase which occurs in two forms: one associated with glucose repression and one constitutively expressed. All of the *F. graminearum* invertase genes are expressed during growth in planta and in vitro. Functional analysis of these genes will reveal their specific roles.

Interestingly, there was a noticeable shift in the relative amounts of the compatible osmolytes trehalose and mannitol in the water-soluble extracts from culture during development (Table 3). At 96 h, the relative trehalose fraction more than doubled and the mannitol fraction decreased by nearly 34%. The 96-h stage is characterized by rapid perithecium expansion and ascus development, whereas the 24-h stage in culture represents the stage at which the fungus begins to go dormant for overwintering in planta or prepares to make perithecia in vitro (Guenther and Trail 2005). Mannitol, trehalose, and glycerol are associated with heat, salt, desiccation, and freezing tolerance in yeasts (Hohmann 2002; Managbanag and Torzilli 2002) and other fungi (Tibbett et al. 2002) because of their capacity to protect membranes and enzymes from damage. There appears to be some preference for the use of one particular compatible osmolyte for a given stress type (Managbanag and Torzilli 2002). Thus, the presence of mannitol at the 24- and 48-h stages in this study indicates that mannitol may be the primary protectant during overwinter dormancy. This may also be reflected in the increase of mannitol to nearly 8% in the senesced wheat stems (Table 3), where the fungus is beginning to go dormant. The increase in trehalose at 96 h may reflect its use as a protectant and as a storage carbohydrate in spores. Interestingly, glycerol is nearly absent from the stages analyzed in Table 3, which indicates that it is not important as a compatible solute during these stages.

Two genes are annotated as malate dehydrogenase (oxaloacetate decarboxlyating; also called $NADP^+$-malic enzyme) in the *F. graminearum* genome. The expression profile of FGSG_07191 (gene 43) (Table 2; Fig. 2) clusters in group 1 (Fig. 2) with the fatty acid synthase genes, whereas FGSG_00805 (gene 40) (Table 2; Fig. 2) falls into group 5 (Fig. 2) with genes from several different categories but clusters tightly with FGSG_02502 (gene 1) (Table 2; Fig. 2), annotated as a sterol delta 5,6 desaturase. The activity of malate dehydrogenase has been correlated with lipid accumulation in *Mortierella alpina* (Wynn et al. 2001; Zhang and Ratledge 2008) and is thought to provide the NADPH required for fatty acid biosynthesis via fatty acid synthase and fatty acid desaturases (Kendrick and Ratledge 1992). A third malate dehydrogenase, FGSG_02461 (gene 41) (Table 2; Fig. 2) is involved in the generation of NADH for the respiratory electron chain.

In general, peroxisomal (PEX) genes follow the same trend in expression as the lipid oxidation genes both in vitro and in planta (data not shown). Maggio-Hall and Keller (2004) have shown that β-oxidation of fatty acids takes place both in peroxisomes (branched and very long-chain fatty acids) and in mitochondria (short-chain and long-chain) in *Aspergillus nidulans*. In contrast, β-oxidation in yeasts takes place only in peroxisomes. The division between the two organelles seems to be the case for most filamentous fungi based on the conservation of genes in available genome sequences (Maggio-Hall et al. 2008) and on studies in specific species (Reich et al. 2009). However, despite the presence of genes for mitochondrial β-oxidation in *Magnaporthe grisea*, it is apparently unable to grow on short-chain fatty acids (Wang et al. 2007), an indication that the presence of genes may not indicate their activity. In *F. graminearum*, the presence of homologues of the *A. nidulans* mitochondrial pathway genes *echA* (enoyl-CoA hydratase, FGSG_00704; gene 16) (Table 2; Fig. 2) and *scdA* (short chain acyl-CoA dehydrogenase, FGSG_09661; gene 23) (Table 2; Fig. 2) indicates the presence of this pathway. These genes, involved in mitochondrial lipid oxidation, show expression typical of lipid oxidation genes (Fig. 2). The PEX genes acyl-coA oxidase (FGSG_02287; gene 18) (Table 2; Fig. 2) and the multifunctional β-oxidation protein (FGSG_09643; gene 22) (Table 2; Fig. 2) have the PST1 PEX signal peptides (AKL and SKL, respectively) associated with their C-termini (Gould et al. 1989; McNew and Goodman 1996) but lack the PST2 N-terminal sequences of other PEX proteins (Flynn et al. 1998; Lammers et al. 2001). The PEX β-oxidation multifunctional protein in *M. grisea* was shown to be localized in peroxisomes despite the absence of any signaling sequences (Wang et al. 2007). Peroxin proteins have been implicated in conidial germination and development in *F. graminearum* by Seong and associates (2008), who observed expression of the PEX genes and β-oxidation genes (those associated with both mitochondria and peroxisomes) during conidial development. The majority of peroxin genes exhibit an expression profile during sexual development similar to that shown by genes involved in lipid oxidation.

The isocitrate lyase gene (FGSG_09896; gene 52) (Table 2; Fig. 2) and the malate synthase gene (FGSG_08700; gene 51) (Table 2; Fig. 2) are indicative of the glyoxylate cycle and, in the mycorrhizal fungus *Glomus intraradices*, the proteins carry PEX targeting signals (Lammers et al. 2001). Only malate synthase has a predicted target peptide, PST1. Interestingly, expression of these genes clusters with that of the lipid biosynthesis genes (Fig. 2), despite their role in the conversion of fats to carbohydrates. A closer examination of their expression patterns reveals a pattern similar to that of the lipid biosynthesis genes in the 0- and 24-h in vitro samples but displays a higher relative level of mRNA for the 48- to 144-h stages, particularly for the isocitrate lyase gene. In planta, levels are reduced for both genes over the early stages compared with the lipid biosynthesis genes. The overall trend toward reduced mRNA accumulation in the in planta stages versus the in vitro stages suggests a difference in the use of the glyoxylate pathway between the two growth conditions. In arbuscular mycorrhizal fungi, it has been previously shown that the glyoxylate cycle is active in the extraradical mycelium (Lammers et al. 2001), whereas lipid biosynthesis predominates within the intraradical mycelium (fungal structures within host roots). Lipids are exported to the extraradical mycelium (Bago et al. 2002), where the glyoxylate cycle is active in utilizing lipid breakdown products for the biosynthesis of carbohydrates (Pfeffer et al. 1999). If mycelia associated with the agar medium were synthesizing lipids and moving them to the aerial mycelia as carbon reserves during the 0- to 24-h stages, then both pathways would be present during vegetative growth. In planta, this division is not necessary because all mycelia are in contact with the plant; or, if it did exist in different host tissues, we would not have observed it in these studies, because plant tissues were not analyzed separately.

These studies were performed using wheat stalks rather than wheat heads. Stalk tissue provided an ideal opportunity for expression analyses because the tissue is more uniform than head tissue and stages of colonization (and development) can be separated as the infection progresses down the stalk. *F. graminearum* commonly colonizes stalks, and stalks form the majority of crop residue after harvest. Therefore, stalks represent an important link between the previous year's crop and the new crop, supporting development of the primary inoculum for the disease. Previously, we investigated the process of colonization of wheat stems (Guenther and Trail 2005) and identified a binucleate stage associated with rapid stalk colonization. In addition, we showed that perithecia were formed in association with stomata and silica cells. The expression data presented here took advantage of this progression to separate stages of development. The signals that drive development of the fungus, particularly in the wheat stalks, are not well understood. Depletion of nitrogen sources has been associated with initiation of sexual development in several fungi (Kent et al. 2008) and with the accumulation of lipids in *Mortierella circinelloides* and *M. alpina* (Ratledge and Wynn 2002; Wynn et al. 2001). In the latter case, growth is limited but carbon assimilation continues and triacylglycerides accumulate in the cells (Ratledge and Wynn 2002). In our study, both lipid accumulation and sexual development occurred in planta in tissue that had been heavily colonized by the fungus and was likely to have a high C:N ratio. Similarly, in vitro sexual development occurred following complete colonization of the carrot agar, which would presumably also be severely depleted in nutrients and likely to have a high C:N ratio. In the field, the lipids are then used for overwintering and as a carbon source for the formation of ephemeral perithecia during warmer temperatures. The association of the perithecia with stomatal cavities suggests the possibility that light or CO_2 may also play a role. These possibilities are currently under study.

In our studies, the lipid bodies formed in hyphae on SC medium, which contains sucrose as the sole carbon source, indicating that the lipids we observed accumulating in hyphae during sexual development were generated de novo. The pattern of gene expression shown in Figure 2 indicates strong co-regulation of genes involved in lipid metabolism and closely follows the pattern of appearance and utilization of lipid bodies. Sequence analyses are in progress to determine possible regulatory genes coordinating expression of both TAG biosynthesis and TAG oxidation. We are addressing our initial hypothesis that lipid accumulation and subsequent utilization are essential for sexual development and overwinter survival. Toward this end, we are performing functional analyses to understand how lipid accumulation and utilization affects sexual development.

MATERIALS AND METHODS

Fungal strains and growth conditions.

F. graminearum strain PH-1 (NRRL 31084, FGSC 9075) was used for all experiments. Stocks were maintained on soil at –20°C. For inoculation of cultures and plants, conidia were generated in carboxymethylcellulose medium (Cappellini and Peterson 1965) and stored at –80°C in 35% glycerol until use. To induce sexual development, petri dishes (60 mm in diameter) containing carrot agar (Klittich and Leslie 1988) were inoculated by spreading 10 µl of conidial suspension (10^5 conidia/ml) across the surface of the agar and incubated at room

temperature (RT; 22 to 24°C) with 24 h of fluorescent lighting for 4 days. Perithecium production was induced as previously described (Bowden and Leslie 1999) by removing a portion of the aerial vegetative hyphae with a toothpick and applying 1 ml of 2.5% Tween 60 (Sigma-Aldrich, St. Louis) to the culture surface, then matting the remaining mycelia with a sterile glass rod. Aerial vegetative hyphae were harvested for analysis by gently scraping mycelia off the surface with a sterile scalpel, minimizing the amount of agar removed. Aerial vegetative hyphae were used because vegetative hyphae are very sparse, and embed within the agar, and were not easily available for harvest. This contrasts with the hyphae of the sexual cycle, which form on the surface of the agar. Induced samples were similarly collected 24, 48, and 96 h after induction. These time points corresponded to important developmental time points delineated by Hallen and associates (2007) as follows: 24 h, wide binucleate hyphae and perithecium initials; 48 h, small perithecia; 72 h, asci initiating; and 96 h, asci developing inside immature perithecia (Hallen et al. 2007). At time point 144 h, the perithecia contain mature spores, which are being forcibly discharged. Collected material was flash frozen and stored at –80°C. Equivalent amounts of carrot agar were also harvested as uninoculated controls.

Wheat cultivation and inoculation.

Spring wheat (*Triticum aestivum* L.) cv. Norm (sugar and lipid analyses) and cv. Bobwhite (Affymetrix Chip analyses) were grown from seed in the greenhouse with supplemental lighting (23°C, 16 h of light and 8 h of darkness). Florets were inoculated as described by Guenther and Trail (2005), with the addition of 10 µl of 10^5 conidia/ml to a single floret per plant near anthesis. Control plants were similarly mock inoculated with water. Stems were harvested by clipping at the base and just below the head. Plants were harvested from the greenhouse approximately 17 days after inoculation for the sugar and lipid analyses and microarray analyses. At this stage, symptoms had progressed an average of half the distance down the topmost internode. For microarray analysis, segments of stem corresponding to the three infection stages were lyophilized and maintained at –80°C until RNA extraction. Tissue from uninfected control plants was isolated from corresponding regions of the stem. To study perithecium development in the stems required greenhouse growth until the entire stem was senesced. The stalk was cut at the base and allowed to air dry for 2 weeks at RT. Stalks were then cut into 7-cm segments and placed in moist vermiculite in glass petri dishes at RT. When perithecia began to produce pigment (after approximately 3 days of incubation), the stems were harvested and stored at –80°C until RNA extraction.

Quantification of sugar uptake in axenic culture.

Uptake of simple sugars by the fungus was performed in Czapek-Dox broth (Stevens 1981), a defined synthetic medium, amended with ^{14}C-labeled sugars as previously described (Bücking and Shachar-Hill 2005). Cultures were grown in 7 ml of medium in 60-mm petri dishes and [U-^{14}C]glucose, [U-^{14}C] sucrose, or [U-^{14}C] fructose (Sigma-Aldrich) constituted a portion of the total sugar. The medium contained 55.49 mM glucose (0.762 µM as [U-^{14}C] glucose with a specific activity of 3 mCi mM^{-1}), 55.49 mM fructose (0.793 µM as [U-^{14}C] fructose with a specific activity of 306 mCi mM^{-1}), or 29.21 mM or 55.49 mM sucrose (0.222 µM as [U-^{14}C] sucrose with a specific activity of 601 mCi mM^{-1}). Each petri dish was inoculated with approximately 500 freshly harvested conidia. The carbohydrate uptake was determined by removing a sample from each treatment (n = 5) at 2, 8, 24, 48, 72, 96, 120, and 144 h after conidia were added, and by comparing the residue of sugars in the medium to uninoculated controls (n = 5). The samples were suspended in a scintillation cocktail (Biosafe II; RPI Corp., Mount Prospect, IL, U.S.A.) and the carbohydrate residue in the solution was quantified using a liquid scintillation counter (LS 6500; Beckman Coulter, Fullerton, CA, U.S.A.).

NMR and GC analysis of sugars.

Tissue samples from carrot agar culture and wheat plants were ground to the consistency of flour in liquid nitrogen with 0.30 g of Superbrite glass beads (3M Corp., St. Paul, MN, U.S.A.) in a mortar with 3 to 5 ml of methanol/water (70:30, vol/vol) as adapted from Pfeffer and associates (1999). This method extracts monosaccharides, disaccharides, oligosaccharides, amino acids, small organic acids, and traces of phospholipids. Samples were filtered through Whatman no. 1 filter paper (Whatman, Middlesex, U.K.). The concentrated extract was lyophilized and stored at –80°C until the time of NMR analysis. For analysis, extracts were resuspended in D_2O. Insoluble particles were removed by centrifugation at 14,000 × g.

NMR analyses of aqueous extracts were performed with a Varian Unity+ 500 MHz spectrometer equipped with a 5-mm NALORAC PFG ^{14}C-^{1}H switchable probe and interfaced with a Sun Microsystems Ultra5 UNIX console. Fully relaxed ^{1}H NMR-FID were acquired, zero filled, and multiplied by an exponential function prior to Fourier transformation to improve the signal-to-noise ratio. NMR peak assignments for trehalose, mannitol, glucose, fructose, and sucrose was performed using literature values (Shachar-Hill and Pfeffer 1996) and by comparison to spectra of authentic reference samples.

Following NMR analysis, 10 µl of each sample was removed and diluted in GC-grade distilled water. Culture samples were diluted 100-fold whereas wheat stem samples were diluted 10-fold. From each diluted sample, 10 µl was removed and dried under nitrogen in a 200-µl insert within a GC vial. To each analyzed sample, 25 µl of methoxyamine HCl in pyridine was added and samples were incubated for 2 h at 50°C following Duran and associates (2003). Samples were mixed by vortexing; then, 25 µl of *N*-methyl-*N*-trimethylsilyl-trifluoroacetamide + 1% trimethylchlorosilane in pyridine was added and incubated at 50°C for 1 h. Samples were mixed by vortexing and 1 µl was injected with a ratio of 25:1 into an Agilent 6890 series gas chromatograph equipped with a 60-m DB-5 MS column (0.32 mm by 0.25 µm) split mode. Injection temperature was maintained at 250°C and the interface temperature was 280°C. The temperature program started with 5 min of isothermal heating at 50°C, followed by a 5°C min^{-1} oven ramp to 315°C and holding at the final 315°C for 10 min (Duran et al. 2003). MS analysis was performed in scan and positive EI mode using an Agilent 5973 series quadrupole mass spectrometer (Agilent Technologies, Palo Alto, CA, U.S.A.). The mass of each sugar was calculated by comparison to the mass of the internal standard.

Lipid extraction and analysis.

For lipid extraction, samples were lyophilized and similar amounts of each sample were combined. Each sample represents the mean of three biological replicates that were combined to obtain sufficient material for NMR analysis. Because technical replicates of GC-FID show very little variation (Li et al. 2006), pooling biological samples was deemed sufficient for both of these techniques. Following lyophilization, the culture samples were ground in a mortar with 0.30 g of Superbrite glass beads (3M) and the infected wheat stems were ground in a small coffee grinder. Each ground sample was extracted in 20 ml of boiling isopropyl alcohol for 30 min (adapted from Pfeffer and associates [1999]). This suspension was filtered through Whatman no. 1 filter paper and evaporated under a

nitrogen stream. The dried residues were resuspended in chloroform, filtered, and again evaporated under a nitrogen stream. Resuspension and drying was repeated using hexanes as the solvent and the sample was finally dissolved in $CDCl_3$ for NMR analysis. Following NMR analysis by one-dimensional ^{1}H-spectroscopy (as above), samples were dried under nitrogen and stored at –20°C in prerinsed glass vials with Teflon-lined screw caps.

NMR samples of stored lipid extracts were derivatized into fatty acid methyl esters and analyzed by GC as follows. Extracts were dissolved in 1 ml of hexane and 40 to 100 µl were analyzed by GC-FID following the protocol of Li and associates (2006). Samples were transferred to prerinsed glass vials (13 by 100 mm) and dried under N_2. To each vial, 2 ml of 5% (vol/vol) concentrated sulfuric acid in methanol (prepared fresh), 25 µl of 0.2% (wt/vol) butylated hydroxytoluene in methanol, and 100 to 400 µg of triheptadecanoin (internal standard) was added. The vials were then closed with Teflon-lined caps, vortexed, and heated to 95°C for 2 h. After cooling to room temperature, 3 ml of 0.9% (wt/vol) NaCl was added and fatty acid methyl esters (FAME) were extracted twice with 2 ml of hexanes. Pooled extracts were evaporated under nitrogen and dissolved in 400 µl of hexane. FAME extracts were analyzed using GC with a flame ionization detector on a DB23 column (30 m, 0.25 mm i.d., 0.25-µm film) (J&W Scientific, Folsom, CA, U.S.A.). Split-mode injection (1:20) was used for GC analysis with the following parameters: injector and flame ionization detector temperature, 260°C; oven temperature program, 140°C for 3 min, then increasing at 10°C min^{-1} to 240°C, and holding for 4 min at that temperature.

Calculation of lipid content was performed following the procedure of Li and associates (2006). The area under the curve for each peak on the GC chromatogram was first corrected for a response factor of the flame ionization detector that differed for each FAME (Christie 1991) and then used to calculate the mass of each FAME in the samples by comparison with the mass of the internal standard. Additionally, a correction for the conversion of FAME weight to TAG weight was used. Moles TAG were calculated from the weight and molecular weight of each FAME. Finally, the TAG content was calculated from the formula Percent TAG by weight = 100 × ([4 × total mol FAME/3] + total g FAME)/g tissue (4 is the molecular weight difference between TAG and three moles of FAME).

Histological procedures.

To visualize lipid bodies, cultures were grown on Synthetic Crossing Medium (Mitchell 1947), as described above, except that plates were center inoculated and no induction with Tween 60 was necessary on this medium to induce sexual development. Vegetative hyphae and hyphae in early stages of sexual development were removed from the agar and stained in squash mounts with aqueous Nile Red (2.5 µg/ml) and incubated for 15 min, followed by two short rinses. Observations were done on a Leica DMRA2 microscope using a Q-capture camera control software (Q-imaging). Nile red fluorescence was viewed using a mercury bulb as a light source, a 450- to 500-nm band pass excitation filter, and a 528-nm-long pass barrier filter.

Affymetrix GeneChip analysis.

The *F. graminearum* Affymetrix GeneChip (Gueldener et al. 2006) was used to study developmental stages in vitro (Hallen et al. 2007) and in planta (this study). Frozen stem samples were lyophilized, ground in a coffee grinder, and homogenized in liquid nitrogen with a mortar and pestle. The RNA was extracted as previously described (Hallen et al. 2007). CEL files were normalized in the Bioconductor package of R version 2.3.0rc (Gentleman et al. 2004; R Development Core Team 2006) using RMA, an expression measure that accounts for background correction, quantile normalization, and variation between arrays (Irizarry et al. 2003a and b). Three biological replicates were analyzed for each treatment. To obtain enough tissue for extractions, multiple stems from the same experiment were pooled for each sample. Affymetrix results are available at Plexdb. All gene numbers are given according to the annotation FG3 on MIPS. Corresponding Affymetrix probe numbers can also be found on the MIPS website.

Comparisons between 48- and 24-h time points were conducted using the Limma package in Bioconductor (Smyth 2005). Statistical significance was empirically determined by selecting the cutoff P value ($P > 0.004$) lower than the smallest P value found in any of the Affymetrix control probesets, as recommended by Smyth (2005).

qRT-PCR.

In order to validate the Affymetrix results, we performed qRT-PCR on four representative genes for three replicates of each time point of the in vitro time course. Primers were designed for fatty acid synthase gene FGSG_05321 (F: 5′ CTTC TCCGTCACCTCTTTCG 3′; R: 5′ GGTCGTCAGCGTAAGG AGAG 3′), triacylglyceride lipase gene FGSG_05906 (F: 5′ A ATCTGCGAGTTGGTGGAAC 3′; R: 5′ GTTCGTAACGCG GAACTCTC 3′), ATP citrate lyase gene FGSG_06039 (F: 5′ TT ATCCCCAACGAGGACAAG 3′; R: 5′ TCCATAGGAGGACC AGCATC 3′), and acyl-CoA dehydrogenase gene FGSG_10790 (F: 5′ CCTTTGGAAGAAGCTCATC 3′; R: 5′ GTAGAGTCG CTCGACCTTGG 3′). The housekeeping gene for glyceraldehyde phosphate dehydrogenase (GAPDH: FGSG_6257; F: 5′ CTACATGCTCAAGTACGACTCTTCC 3′; R: 5′ GCCGGTC TCGGACCACTTG 3′) was used as a control. RNA (100 µg) from the same extractions as used for the Affymetrix GeneChip was treated with 10 U of RNase-free DNase (Roche, Mannheim, Germany) for 15 min, followed by cleanup using the RNeasy mini kit (Qiagen, Valencia, CA, U.S.A.) following the manufacturer's instructions (for the 24-h time point, fresh RNA was collected as described above). Single-stranded cDNA was synthesized using AffinityScript cDNA master mix (Agilent), and qRT-PCR reactions were set up using Brilliant II SYBR Green QPCR master mix (Agilent Technologies, Santa Clara, CA, U.S.A.), following the manufacturer's instructions. All reactions included a no-reverse transcriptase control. Reactions (25 µl) were run on an ABI Prism 7000 Sequence Detection System, running ABI 7000 System SDS Software (Applied Biosystems, Foster City, CA, U.S.A.) for 40 cycles, following standard protocols. Expression analysis was performed by determining the ratio of CtGAPDH to the Ct for each gene.

ACKNOWLEDGMENTS

We thank D. David for technical assistance, E. Collakova and D. Allan for assistance with the lipid analyses, and M. T. Rogers at the Michigan State University NMR facility. This research was supported, in part, by the United States Department of Agriculture (USDA) under Agreement No. 59-0790-6-068, a cooperative project with the United States Wheat & Barley Scab Initiative; by a grant from the National Research Initiative of the USDA Cooperative State Research, Education and Extension Service (grant no. 2004-35604-14327 to F. Trail); and by the Michigan Agricultural Experiment Station.

LITERATURE CITED

Acevedo, E., Fereres, E., Hsaio, T. C., and Henderson, D. W. 1979. Diurnal growth trends, water potential and osmotic adjustment of maize and sorghum. Plant Physiol. 67:476-480.

Bagnat, M., Keranen, S., Shevchenko, A., Shevchenko, A., and Simons, K. 2000. Lipid rafts function in biosynthetic delivery of proteins to the cell surface in yeast. Proc. Natl. Acad. Sci. U.S.A. 97:3254-3259.

Bago, B., Zipfel, W., Williams, R. M., Jun, J., Arreola, R., Lammers, P. J., Pfeffer, P. E., and Shachar-Hill, Y. 2002. Translocation and utilization of fungal storage lipid in the arbuscular mycorrhizal symbiosis. Plant Physiol. 128:108-124.

Bao, X. M., Katz, S., Pollard, M., and Ohlrogge, J. 2002. Carbocyclic fatty acids in plants: Biochemical and molecular genetic characterization of cyclopropane fatty acid synthesis of *Sterculia foetida*. Proc. Natl. Acad. Sci. U.S.A. 99:7172-7177.

Bowden, R. L., and Leslie, J. F. 1999. Sexual recombination in *Gibberella zeae*. Phytopathology 89:182-188.

Bücking, H., and Shachar-Hill, Y. 2005. Phosphate uptake, transport and transfer by the arbuscular mycorrhizal fungus *Glomus intraradices* is stimulated by increased carbohydrate availability. New Phytol. 165:899-912.

Calvo, A. M., Hinze, L. L., Gardner, H. W., and Keller, N. P. 1999. Sporogenic effect of polyunsaturated fatty acids on development of *Aspergillus* spp. Appl. Environ. Microbiol. 65:3668-3673.

Calvo, A. M., Gardner, H. W., and Keller, N. P. 2001. Genetic connection between fatty acid metabolism and sporulation in *Aspergillus nidulans*. J. Biol. Chem. 276:25766-25774.

Cappellini, R., and Peterson, J. 1965. Macroconidium formation in submerged cultures by a non-sporulating strain of *Gibberella zeae*. Mycologia 57:962-966.

Carlson, M., and Bodstein, D. 1982. Two differentially regulated mRNAs with different 5′ ends encode secreted with intracellular forms of yeast invertase. Cell 28:145-154.

Carpenter, G., and Ji, Q. S. 1999. Phospholipase C-gamma as a signal-transducing element. Exp. Cell Res. 253:15-24.

Chen, X. M., and Yuan, C. 1984. Application of microcomputer in studying wheat scab epidemiology and forecasting. Zhejiang Agric. Sci. 2:55-60.

Cheng, C. S., Samuel, D., Liu, Y. J., Shyu, J. C., Lai, S. M. Lin, K. F., and Lyu, P. C. 2004. Binding mechanism of nonspecific lipid transfer proteins and their role in plant defense. Biochemistry 43:13628-13636.

Christie, W. W. 1991. Recent developments in high-performance liquid and gas-chromatography of lipids. Rev. Fr. Corps Gras 38:155-160.

Desjardins, A. E., Plattner, R. D., Shaner, G., Brown, D. W., Buechley, G., Proctor R. H., and Turgeon, G. G. 2006. Field release of *Gibberella zeae* genetically modified to lack ascospores. Page 39-44 in: Fusarium Head Blight Forum. S. M. Canty, A. Clark, and D. Van Sanford, eds. University of Kentucky, Research Triangle Park, NC, U.S.A.

Duran, A. L., Yang, J., Wang, L. J., and Sumner, L. W. 2003. Metabolomics spectral formatting, alignment and conversion tools (MSFACTs). Bioinformatics 19:2283-2293.

Dyer, P. S., Ingram, D. S., and Johnstone, K. 1993. Evidence for the involvement of linoleic-acid and other endogenous lipid factors in perithecial development of *Nectria haematococca* mating population 6. Mycol. Res. 97:485-496.

Flynn, C. R., Mullen, R. T., and Trelease, R. N. 1998. Mutational analyses of a type 2 peroxisomal targeting signal that is capable of directing oligomeric protein import into tobacco BY-2 glyoxysomes. Plant J. 16:709-720.

Gentleman, R. C., Carey, V. J., Bates, D. M., Bolstad, B., Dettling, M., Dudoit, S., Ellis, B., Gautier, L., Ge, Y. C., Gentry, J., Hornik, K., Hothorn, T., Huber, W., Iacus, S., Irizarry, R., Leisch, F., Li, C., Maechler, M., Rossini, A. J., Sawitzki, G., Smith, C., Smyth, G., Tierney, L., Yang, J. Y. H., and Zhang, J. H. 2004. Bioconductor: Open software development for computational biology and bioinformatics. Genome Biol. 5:R80.

Gould, S. J., Keller, G. A., Hosken, N., Wilkinson, J., and Subramani, S. 1989. A conserved tripeptide sorts proteins to peroxisomes. J. Cell Biol. 108:1657-64.

Gueldener, U., Seong, K. Y., Boddu, J., Cho, S. H., Trail, F., Xu, J.-R., Adam, G., Mewes, H. W., Muehlbauer, G., and Kistler, H. C. 2006. Development of a *Fusarium graminearum* Affymetrix GeneChip for profiling fungal gene expression in vitro and in planta. Fungal Genet. Biol. 43:316-325.

Guenther, J. C., and Trail, F. 2005. The development and differentiation of *Gibberella zeae* (anamorph: *Fusarium graminearum*) during colonization of wheat. Mycologia 97:229-237.

Hallen, H. E., Huebner, M., Shiu, S.-H., Guldener, U., and Trail, F. 2007. Gene expression shifts during perithecium development in *Gibberella zeae* (anamorph *Fusarium graminearum*), with particular emphasis on ion transport proteins. Fungal Genet. Biol. 44:1146-1156.

Hohmann, S. 2002. Osmotic stress signaling and osmoadaptation in yeasts. Microbiol. Mol. Biol. Rev. 66:300-371.

Ikeda, T., Higashi, S., and Ono, S. 1955. Studies on the resistance of wheat and barley varieties to ear scab disease (*Gibberella zeae*). III. Studies on varietal difference in relation to the enlargement of spots. Bull. Div. Plant Breed. Tokai-Kinki Agric. Stn. 2:69-75.

Inch, S., Fernando, W. G. D., and Gilbert, J. 2005. Seasonal and daily variation in the airborne concentration of *Gibberella zeae* (Schw.) Petch spores in Manitoba. Can. J. Plant Pathol. 27:357-363.

Irizarry, R. A., Hobbs, B., Collin, F., Beazer-Barclay, Y. D., Antonellis, K. J., Scherf, U., and Speed, T. P. 2003a. Exploration, normalization, and summaries of high density oligonucleotide array probe level data. Biostatistics 4:249-264.

Irizarry, R. A., Bolsta, B M., Collin, F., Cope, L. M., Hobbs, B., and Speed, T. P. 2003b. Summaries of Affymetrix GeneChip probe level data. Nucleic Acids Res. 31:e15.

Istokovics, A., Morita, N., Izumi, K., Hoshino, T., Yumoto, I., Sawada, M. T., Ishizaki, K., and Okuyama, H. 1998. Neutral lipids, phospholipids, and a betaine lipid of the snow mold fungus *Microdochium nivale*. Can. J. Microbiol. 44:1051-1059.

Jones, M. M., Osmond, C. B., and Turner, N. C. 1980. Accumulation of solutes in leaves of sorghum and sunflower in responses to water deficits. Aust. J. Plant Physiol. 7:193-205.

Kameli, A., and Losel, D. M. 1996. Growth and sugar accumulation in durum wheat plants under water stress. New Phytol. 132:57-62.

Kendrick, A., and Ratledge, C. 1992. Desaturation of polyunsaturated fatty acids in *Mucor circinelloides* and the involvement of a novel membrane-bound malic enzyme. Eur. J. Biochem. 209:667-673.

Kent, C. R., Ortiz-Bermudez, P., Giles, S. S., and Hull, C. M. 2008. Formulation of a defined V8 medium for induction of sexual development of *Cryptococcus neoformans*. Appl. Environ. Microbiol. 74:6248-6253.

Klittich, C. J. R., and Leslie, J. F. 1988. Nitrate reduction mutants of *Fusarium moniliforme* (*Gibberella fujikuroi*). Genetics 118:417-423.

Lammers, P. J., Jun, J., Abubaker, J., Arreola, R., Gopalan, A., Bago, B., Hernandez-Sebastia, C., Allen, J. W., Douds, D. D., Pfeffer, P. E., and Shachar-Hill, Y. 2001. The glyoxylate cycle in an arbuscular mycorrhizal fungus. Carbon flux and gene expression. Plant Physiol. 127:1287-1298.

Li, Y., Beisson, F., Pollard, M., and Ohlrogge, J. 2006. Oil content of *Arabidopsis* seeds: The influence of seed anatomy, light and plant-to-plant variation. Phytochemistry 67:904-15.

Maggio-Hall, L. A., and Keller, N. P. 2004. Mitochondrial beta-oxidation in *Aspergillus nidulans*. Mol. Microbiol. 54:1173-1185.

Maggio-Hall, L. A., Lyne, P., Wolff, J. A., and Keller, N. P. 2008. A single acyl-CoA dehydrogenase is required for catabolism of isoleucine, valine and short-chain fatty acids in *Aspergillus nidulans*. Fungal Genet. Biol. 45:180-9.

Managbanag, R. R., and Torzilli, A. P. 2002. An analysis of trehalose, glycerol and mannitol accumulation during heat and salt stress in a salt marsh isolate of *Aureobasidium pullulans.* Mycologia 94:384-391.

McNew, J. A., and Goodman, J. M. 1996. The targeting and assembly of peroxisomal proteins: Some old rules do not apply. Trends Biochem. Sci. 21:54-58.

Mitchell, H. K. 1947. *Neurospora*. V. A synthetic medium favoring sexual reproduction. Am. J. Bot. 34:573-577.

Murphy, D. J. 2001. The biogenesis and functions of lipid bodies in animals, plants and microorganisms. Prog. Lipid Res. 40:325-438.

Murphy, D. J., and Vance, J. 1999. Mechanisms of lipid-body formation. Trends Biochem. Sci. 24:109-115.

Pfeffer, P. E., Douds, D. D., Becard, G., and Shachar-Hill, Y. 1999. Carbon uptake and the metabolism and transport of lipids in an arbuscular mycorrhiza. Plant Physiol. 120:587-598.

R Development Core Team. 2006. R: A Language and Environment for Statistical Computing. R Foundation for Statistical Computing, Vienna, Austria.

Ranos-Pamplona, M., and Naqvl, N. I. 2006. Host invasion during rice-blast disease requires carnitine-dependent transport of peroxisomal aceyl-CoA. Mol. Microbiol. 61:61-75.

Ratledge, C., and Wynn, J. P. 2002. The biochemistry and molecular biology of lipid accumulation in oleaginous microorganisms. Pages 1-51 in: Advances in Applied Microbiology, Vol. 51. Academic Press Inc., San Diego, CA, U.S.A.

Reich, M., Gobel, C., Kohler, A., Buee, M., Martin, F., Feussner, I., and Polle, A. 2009. Fatty acid metabolism in the ectomycorrhizal fungus *Laccaria bicolor*. New Phytol. 182:950-964.

Reis, E. M. 1990. Effects of rain and relative humidity on the release of ascospores on the infection of wheat heads by *Gibberella zeae.* Fitopatol. Bras. 15:339-343.

Seong, K. Y., Zhao, X., Xu, J. R., Guldener, U., and Kistler, H. C. 2008. Conidial germination in the filamentous fungus *Fusarium graminearum*. Fungal Genet. Biol. 45:389-99.

Shachar-Hill, Y., and Pfeffer, P. E. 1996. Nuclear Magnetic Resonance in Plant Biology. American Society of Plant Physiologists, Rockville, MD, U.S.A.

Shaner, G. E. 2003. Epidemiology of Fusarium Head Blight of small grain cereals in North America. Pages 84-119 in: Fusarium Head Blight of Wheat and Barley. K. J. Leonard and W. R. Bushnell, eds. American Phytopathological Society Press, St. Paul, MN, U.S.A.

Smyth, G. K. 2005. Limma: Linear models for microarray data. In: Bioinformatics and Computational Biology Solutions Using R and Bioconductor. R. Gentleman, V. Carey, S. Dudoit, R. Irizarry, and W. Huber, eds. Springer, New York.

Stevens, R. B. 1981. Mycology Guidebook. University of Washington Press, Seattle.

Tibbett, M., Sanders, F. E., and Cairney, J. W. G. 2002. Low temperature-induced changes in trehalose, mannitol and arabitol associated with enhances tolerance to freezing in ectomycorrhizal basidiomycetes (*Hebeloma* spp.) Mycorrhiza 12:249-255.

Trail, F. 2009. For blighted waves of grain: *Fusarium graminearum* in the postgenomics era. Plant Physiol. 149:103-110.

Trail, F., and Common, R. 2000. Perithecial development by *Gibberella zeae*: A light microscopy study. Mycologia 92:130-138.

Trail, F., Xu, H. X., Loranger, R., and Gadoury, D. 2002. Physiological and environmental aspects of ascospore discharge in *Gibberella zeae* (anamorph *Fusarium graminearum*). Mycologia 94:181-189.

Tsitsigiannis, D. I., Zarnowski, R., and Keller, N. P. 2004. The lipid body protein, PpoA, coordinates sexual and asexual sporulation in *Aspergillus nidulans*. J. Biol. Chem. 279:11344-11353.

Voegele, R. T., Struck, C., Hahn, M., and Mendgen, K. 2001. The role of haustoria in sugar supply during infection of broad bean by the rust fungus *Uromyces fabae*. Proc. Natl. Acad. Sci. U.S.A. 98:8133-8138.

Voegele, R. T., Wirsel, S., Möll, U., Lechner, M., and Mendgen, K. 2006. Cloning and characterization of a novel invertase form the obligate biotroph *Uromyces fabae* and the analysis of expression patterns of host and pathogen invertases in the course of infection. Mol. Plant-Microbe Interact. 19:625-634.

Walters D. R., Cowley, T., McPherson, A., Marshall, G., and McRoberts, N. 1996. Sugar transport in the light leaf spot pathogen *Pyrenopeziza brassicae*. FEMS (Fed. Eur. Microbiol. Soc.) Microbiol. Lett. 143:285-289.

Wang, Z.-Y., Soanes, D. M., Kersaw, M. J., and Talbot, N. J. 2007. Functional analysis of lipid metabolism in *Magnaporthe grisea* reveals a requirement for peroxisomal fatty acid β-oxidation during appressorium-mediated plant infection. Mol. Plant-Microbe Interact. 20:475-491.

Weete, J. D. 1974. Fungal Lipid Biochemistry; Distribution and Metabolism. Plenum Press, New York,.

Wright D. P., Baldwin, B. C., Shephard, M. C., and Scholes, J. D. 1995. Source-sink relationships in wheat leaves infected with powdery mildew. I. Alterations in carbohydrate metabolism. Physiol. Mol. Plant Pathol. 47:237-253.

Wynn, J. P., Hamid, A. A., Li, Y., and Ratledge, C. 2001. Biochemical events leading to the diversion of carbon into storage lipids in the oleaginous fungi *Mucor circinelloides* and *Mortierella alpina*. Microbiology 147:2857-64.

Zhang, Y., and Ratledge, C. 2008. Multiple isoforms of malic enzyme in the oleaginous fungus, *Mortierella alpina*. Mycol. Res. 112:725-730.

AUTHOR-RECOMMENDED INTERNET RESOURCE

MIPS *Fusarium graminearum* genome database:
mips.helmholtz-muenchen.de/genre/proj/FGDB